Description and modelling of robot-manipulator FANUC M-430iA/4FH

E Nikolov, NG Nikolova, M Georgiev

Technical University-Sofia; FA, DIA; 8, Kliment Ohridski str., Sofia-1000, Bulgaria
nicoloff@tu-sofia.bg, ninan@tu-sofia.bg, georgievmg@tu-sofia.bg

Summary: In this work, you can find the results from the description and modeling of the robotic manipulator FANUC M-430iA / 4FH. The basic values that determine the performance of the robot are tested and analyzed. An analytical model was developed on the basis of which it's temporal and frequency characteristics are illustrated in the absence and availability of maximum mechanical load of the working spherical wrist

1. Introduction.

The purpose of this paper is to explore the possibilities of industrial robotic manipulator FANUC M-430iA/4FH. The work tasks are: description, modeling and visualization of the dynamic characteristics of the robotic manipulator. Fig. 1 shows the construction diagram of industrial robotic manipulator FANUC M-430iA/4FH with anthropomorphic arms, spherical working wrist and five independent motion control axes (5-DOF). The electric drive of the robot is carried out with DC motor with permanent magnet (from FANUC-type servo motors β_i or α_i).

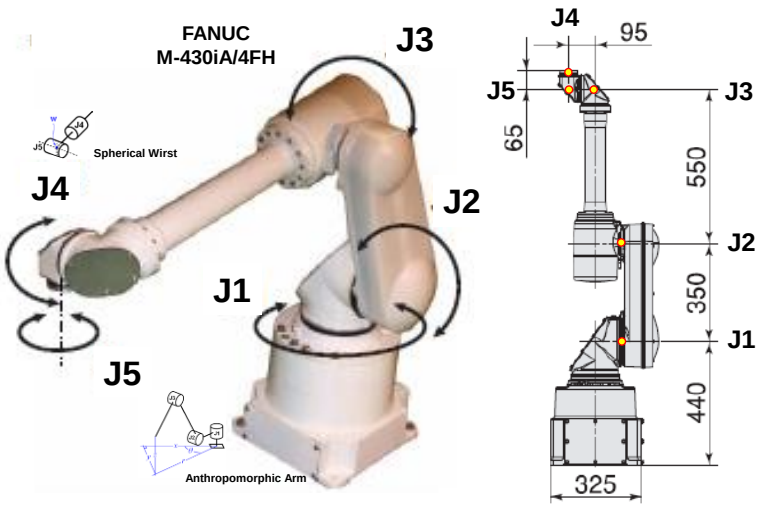

Fig.1. The construction scheme of industrial robotic manipulator FANUC M-430iA/4FH

The mechanical parameters of the robot (rotation ranges and shoulder dimensions, speed, mechanical moments, inertia, maximum lift, energy consumption and power, maximum accuracy, etc.) in the respective dimensions are systematized and presented in Table 1 [12-20].

Tabl.1

5-DOF Robot-Manipulator FANUC M-430iA/4FH, Controlled Axis of Motion 5, Payload 4 kg						
Joint	J_i	**J1**	**J2**	**J3**	**J4**	**J5**
Motion Range	$[^\circ]$	$360\,[^\circ]$	$230\,[^\circ]$	$383\,[^\circ]$	$300\,[^\circ]$	$540\,[^\circ]$
Robot Maximum Speed	$[^\circ/s]$	$300\,[^\circ/s]$	$320\,[^\circ/s]$	$320\,[^\circ/s]$	$360\,[^\circ/s]$	$2000\,[^\circ/s]$
Robot Maximum Speed	$[rad/s]$	$5,24\,[rad/s]$	$5,59\,[rad/s]$	$5,59\,[rad/s]$	$6,28\,[rad/s]$	$34,91\,[rad/s]$
Wirst Moment	$[Nm]$	-	-	-	$3,5\,[Nm]$	$1,5\,[Nm]$
Wirst Moment	$[kgf.m]$	-	-	-	$0,36\,[kgf.m]$	$0,15\,[kgf.m]$
Wirst Inertia	$[kg.m^2]$	-	-	-	$0,064\,[kg.m^2]$	$0,010\,[kg.m^2]$
Wirst Inertia	$[kgf.cm.s^2]$				$0,65$	$0,102$
Length Arm	$[mm]$	$350\,[mm]$	$550\,[mm]$	$95\,[mm]$	$65\,[mm]$	-
Max. Load Capacity an Wirst	$[kg]$	-	-	-	-	$4\,[kg]$
Repeatability	$[mm]$	$\pm 0,5\,[mm]$				
Mechanical Weight Robot Mass	$[kg]$	$55\,[kg]$				
Average Power Consumption	$[kW]$	$1\,[kW]$				
H-Reach	$[mm]$	$900\,[mm]$				
Average Power Consumption	$[kW]$	$1\,[kW]$				

This paper offers and examines a corresponding mathematical model of kinematics of 5-DOF FANUC M-430iA/4FH by Todefine. The kinematic scheme of the axis of the manipulator is presented in Fig. 2 in accordance with the Denavit-Hartenberg method of constructive connection configuration (Fig.1). The following markings are used: z - axis in the direction of the joint; x - axis parallel to the common normal; q_i - the angle from x_{i-1} to x_i along z_{i-1}; d_i - distance from the intersection of z_{i-1} with x_i to the origin of $(i-1)$ - system of axis; a_i - shortcut between z_{i-1} and z_i; α_i angle from z_{i-1} to z_i with length x_i. The kinematic scheme parameters (Fig.2) are shown in Tabl. 2.

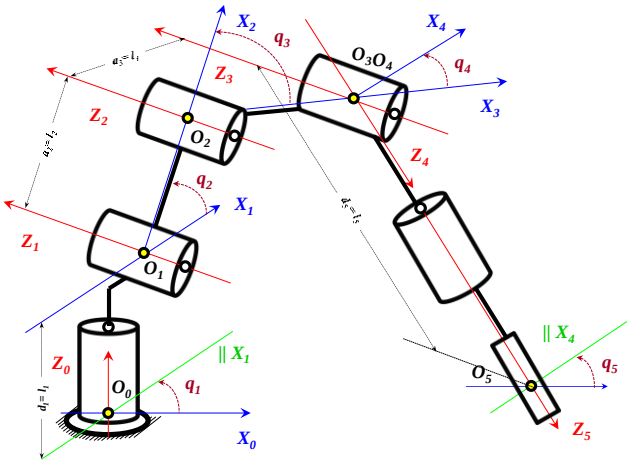

Fig.2. The kinematic scheme of the axis of the manipulator

Tabl.2

Denavit-Hartenberg parameters of the 5-DOF robot-manipulator FANUC M-430iA/4FH				
I	q_i	α_i	a_i	d_i
1	q_1	$-\pi/2$	0	d_1
2	q_2	0	a_2	0
3	q_3	0	a_3	0
4	q_4	$\pi/2$	0	0
5	q_5	0	0	d_5

2. Modeling, parameterization and analysis of the 5-DOF FANUC M-430iA/4FH industrial robotic manipulator.

As an object of control, the industrial robotic manipulator is considered with: input (control) values - control signals $\mu_{Ji}\ (i \in [1,5])$ to the electric motors and output (adjustable) values - positions $y_{Ji}\ (i \in [1,5])$ of the axes of the 5-DOF manipulator. The structural model (Figure 3) is presented in *"**without loading the wrist**"* mode in Fig. 3.b and in operational ***"with max load an wrist"*** mode in Fig. 3.c, where ς_M indicates the mechanical load of the robotic manipulator by the workpiece being machined, and G_i - the transmission functions of the electromechanical propulsion of the arm of the manipulator.

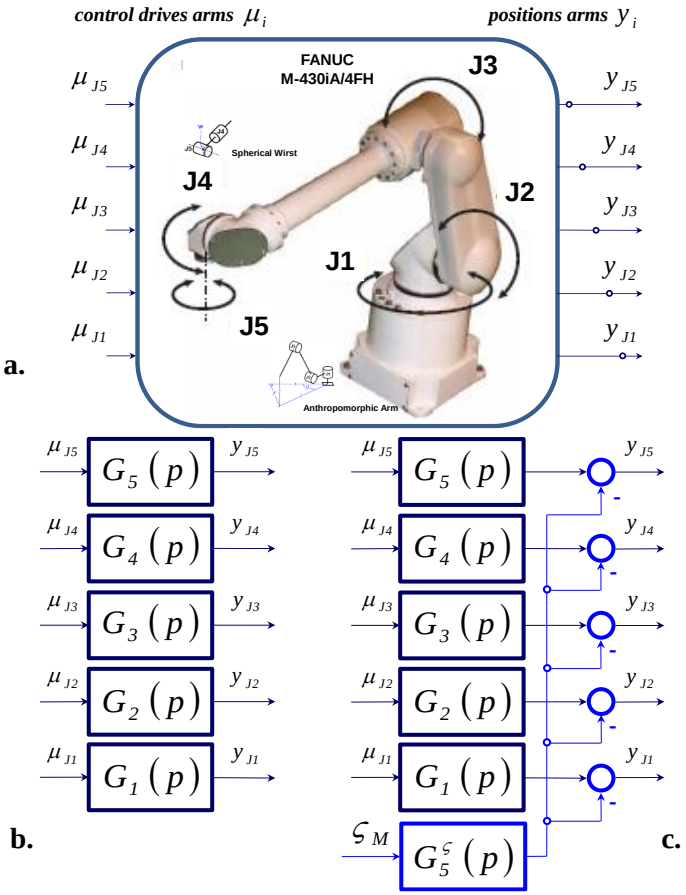

Fig.3. Structured model of 5-DOF FANUC M-430iA/4FH

Literature [1-11] and laboratory studies as well as experimental verification determine the possibilities for analytical modeling of the dynamics of FANUC M-430iA / 4FH in the following sequence. The schematic diagram (Fig. 4) of the electric drive (uniform on all axes of the 5-DOF manipulator) with a DC motor with permanent magnet is considered, where the following markings are used: R_a - anchor resistance; L_a - inductance of scattering; u_a - power supply voltage; i_a - anchor current; T_1 - torque of the motor shaft; T_m - electromagnetic moment of the motor shaft; J_m - inertia moment of the motor; K - current-to-moment ratio; B_m - viscous friction coefficient; ω_m - motor shaft speed; θ_m - shaft position.

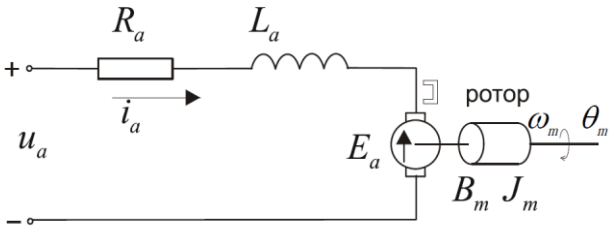

Fig.4. Schematic diagram of the electric drive

The basic equations of analytically describing functional dependencies between the main characterizing variables of the scheme are (1) ÷ (3), and the equations modeling the electrical and mechanical parts are (4) и (5) respectively. After replacing the variables in equations (4) and (5), we reach (6), where T_s is the time constant of the motor and K_{sm} is the gain of the motor. The last two dimensions are determined according to (7):

$$\frac{d}{dt} i_a = \frac{1}{L_a} u_a - \frac{R_a}{L_a} i_a - \frac{K}{L_a} \omega_m \tag{1}$$

$$\frac{d}{dt} \omega_m = \frac{K}{J_m} i_a - \frac{B_m}{J_m} \omega_m - \frac{1}{J_m} T_1 \tag{2}$$

$$\frac{d}{dt} \theta_m = \omega_m \tag{3}$$

$$u_a(t) = R_a i_a(t) + K\omega_m(t) \tag{4}$$

$$J\dot{\omega}_m(t) = K i_a(t) - B_m \omega_m(t) \tag{5}$$

$$T_s \dot{\omega}_m(t) = -\omega_m(t) + K_s u_a(t) \tag{6}$$

$$T_s = \frac{R_a J}{BR_a + K^2} \; ; \; K_{sm} = \frac{K}{BR_a + K^2} \tag{7}$$

With the help of (1) ÷ (7) the transfer functions G_{ω_m} and G_{θ_m} of the robotic manipulator are determined by the speed and by the position of the motor shaft as (8) and (9)

$$G_{\omega_m}(p) = \frac{\omega_m(p)}{u_a(p)} = \frac{K_{sm}}{T_s p + 1} \tag{8}$$

$$G_{\theta_m}(p) = \frac{\theta_m(p)}{u_a(p)} = \frac{K_{sm}}{p(T_s p + 1)} \tag{9}$$

The complete transmission functions (both in speed $G^{\Sigma}_{\omega_m}(p)$ and in position $G^{\Sigma}_{\theta_m}(p)$, $\theta_m \equiv y$) of the electric drive (10), (11) depend both on the supply voltage $u_a \equiv \mu$ and on the moment $M_c \equiv \varsigma_m$ of the mechanical loading of the shaft, which is structurally reflected in Fig. 3.c ., and only by position θ_m - in Fig.5

$$\begin{aligned} G^{\Sigma}_{\omega_m}(p) &= \frac{K_{sm}}{(T_s p + 1)} \frac{u_a(p)}{\omega_m(p)} - \frac{k_c(T_a p + 1)}{(T_{as} p + 1)(T_m p + 1)} \frac{M_c(p)}{\omega_m(p)} \\ \omega_m(p) &= \frac{K_{sm}}{T_s p + 1} u_a(p) - \frac{k_c(T_a p + 1)}{(T_{as} p + 1)(T_m p + 1)} M_c(p) \end{aligned} \tag{10}$$

$$G_{\theta_m}^{\Sigma}(p)=\frac{K_{sm}}{p(T_s p+1)}\frac{u_a(p)}{\omega_m(p)}-\frac{k_c(T_a p+1)}{p(T_{as} p+1)(T_m p+1)}\frac{M_c(p)}{\omega_m(p)}$$
$$\theta_m(p)=\left(\frac{1}{p}\right)\frac{K_{sm}}{T_s p+1}u_a(p)-\left(\frac{1}{p}\right)\frac{k_c(T_a p+1)}{(T_{as} p+1)(T_m p+1)}M_c(p) \quad (11)$$

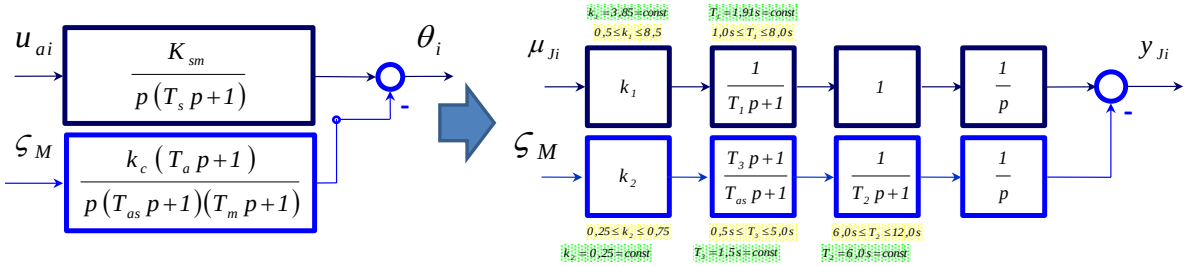

Fig.5. The ranges of parametric fluctuations of the control object

The characteristics (12) ÷ (17) of the control object (Fig.3) are parameterized [1-20], with ranges of parametric fluctuations are indicated and marked in Tabl. 3 and in Fig. 5

Tabl.3

	k_{1nom}	T_{1nom}	k_{2nom}	T_{2nom}	T_{3nom}
	$k_1=3,85$	$T_1=1,91s$	$k_2=0,25$	$T_2=6,0s$	$T_2=1,5s$
	k_1 var	T_1 var	k_2 var	T_2 var	T_3 var
1	3,58	0,5 s	0,253	6 s	1,0 s
2	4,58	1,0 s	0,353	7 s	1,5 s
3	5,58	2,0 s	0,453	8 s	2,0 s
4	6,58	3,0 s	0,553	9 s	3,0 s
5	7,58	4,0 s	0,653	10 s	4,0 s
6	8,58	5,0 s	0,753	11 s	4,5 s

$$G_5=G_{\theta_m}(p)=\frac{\theta_m(p)}{u(p)}=\frac{K_s}{p(T_s p+1)}=\frac{3,58}{p(0,91p+1)} \quad (12)$$
$$G_4=G_{\theta_m}(p)=\frac{\theta_m(p)}{u(p)}=\frac{K_s}{p(T_s p+1)}=\frac{3,58}{p(1,05p+1)} \quad (13)$$
$$G_3=G_{\theta_m}(p)=\frac{\theta_m(p)}{u(p)}=\frac{K_s}{p(T_s p+1)}=\frac{3,58}{p(1,25p+1)} \quad (14)$$
$$G_2=G_{\theta_m}(p)=\frac{\theta_m(p)}{u(p)}=\frac{K_s}{p(T_s p+1)}=\frac{3,58}{p(1,55p+1)} \quad (15)$$
$$G_1=G_{\theta_m}(p)=\frac{\theta_m(p)}{u(p)}=\frac{K_s}{p(T_s p+1)}=\frac{3,58}{p(1,91p+1)} \quad (16)$$
$$G^{\varsigma_M}(p)=-\frac{\theta_m(p)}{\varsigma_M(p)}=-\frac{k_c(T_a p+1)}{p(T_s p+1)(T_m p+1)}=-\frac{0,253(1,5p+1)}{p(0,01p+1)(6p+1)} \quad (17)$$

3. Preview of the parameterized performance models of 5-DOF FANUC M-430iA / 4FH industrial robotic manipulator

The analytical models of the electric drive of the robotic manipulator by position $\theta_m \equiv y$ are simulated in the ranges specified in Tabl.3. The transients $y_i(t)$ (at $u_a = 1(t)$) and impulse transients $i_i(t)$ (at $u_a = \delta(t)$) characteristics of the electric drive of the manipulator are presented respectively in Fig.6 and Fig.7 in "***without loading the wrist***" mode and in "***with max load an wrist***" operational mode. The frequency characteristics $G_{\theta_m}(j\omega)$ of the modeled dynamic system by position are illustrated in Fig.8 in Fig.9 in "***without loading the wrist***" mode and in "***with max load an wrist***" operational mode

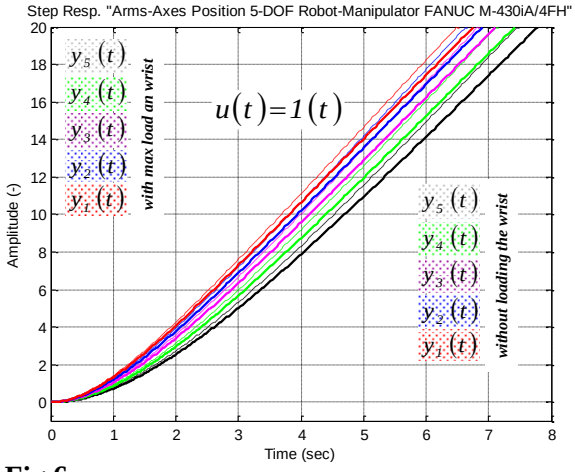

Fig.6.

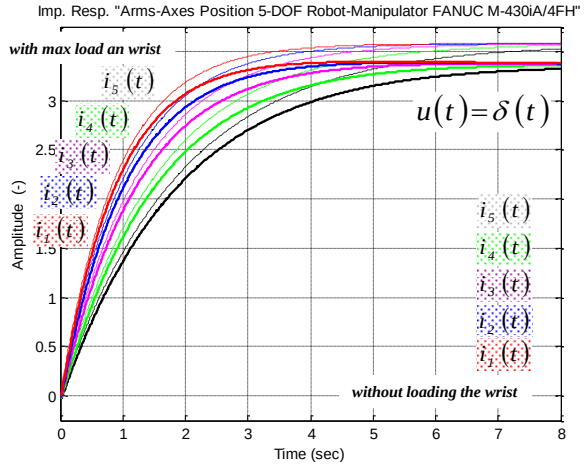

Fig.7.

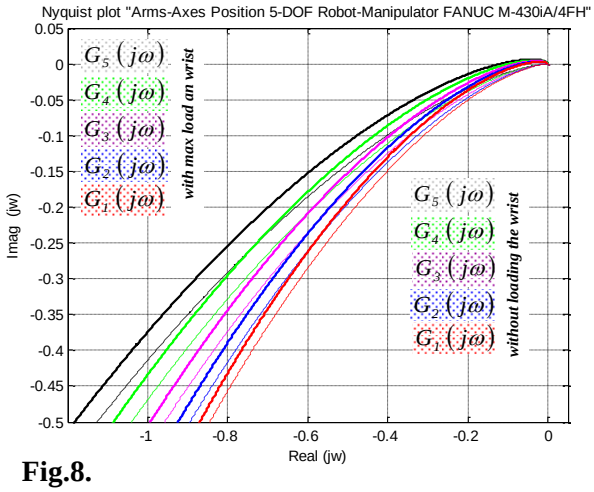

Fig.8.

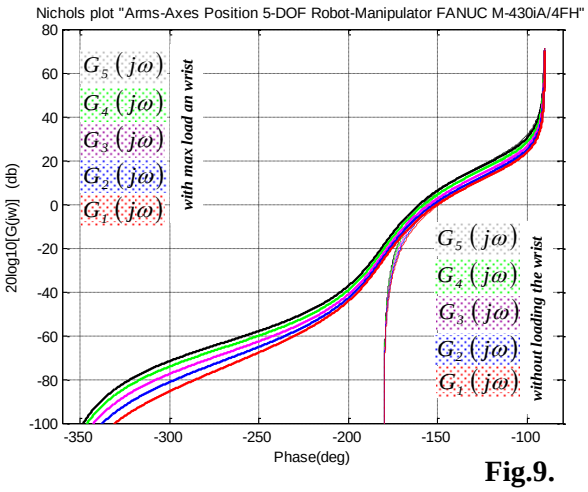

Fig.9.

4. Conclusion

The new and original in this paper is:

■ The proposed description of the structural layout of the 5-DOF industrial robotic manipulator FANUC M-430iA / 4FH, the systematization of the mechanical quantities and parameters of the robot (rotational ranges and dimensions of the arms, speed, mechanical moments, inertia, maximum lifting capacity, energy consumption and power, maximum accuracy, etc.) in the respective dimensions, as well as the developed kinematic scheme of the axes of the manipulator Fig.2 in accordance with the Denavit-Hartenberg method**;**

■ The developed analytical model of the dynamics on the position of the axes of the 5-DOF manipulator in the "without loading the wrist" mode and in the "with max load an wrist" operational mode under the influence of the mechanical load on the robotic manipulator by the workpiece machining dur-

ing the production, as well as the parameterization of the analytical model developed on the basis of literary and laboratory studies and experimental verification**;**

■ The transmission functions are determined by speed and by position of FANUC M-430iA / 4FH as an object in a control system, representing the main characteristics of the manipulator in the synthesis of the system;

■ The proposed analytical models of the industrial robotic manipulator are visualized. It presents its transient, impulse transient and frequency characteristics, defining the FANUC M-430iA / 4FH as a static dynamic speed system and an astatic dynamic motion system

Acknowledgment

The authors would like to thank the Bulgarian National Science Fund for the financial support by project КП-06-Н37/17.

References

1. Abdulrahman A.A.Emhemed, Rosbi Bin Mamat (2012), *Modelling and Simulation for Industrial DC Motor Using Intelligent Control*, Procedia Engineering 41 (2012) 420-425
2. Amir Khazaee, Hosein Abootorabi Zarchi, Gholamreza Arab Markadeh (2019), *Loss model based efficiency optimized control of brushless DC motor drive*, ISA Transactions 86 (2019) 238-248
3. F. S. Ahmed, S. Laghrouche, M. El Bagdouri (2010*), Pancake Type DC Limited Angle Torque Motor: Modeling and Identification, Application to Automobile Air Path Actuators*, 6th IFAC Symposium Advances in Automotive Control Munich, Germany, July 12-14, 2010, 978-3-902661-72-2/10/$20.00 © 2010 IFAC, 10.3182/20100712-3-DE-2013.00135, 431-436
4. Fayez S. Ahmed, Salah Laghrouche, Mohammed El Bagdouri (2012), *Analysis, modeling, identification and control of pancake DC torque motors: Application to automobile air path actuators*, Mechatronics 22 (2012) 195-212
5. M. Ruderman, J. Krettek, F. Hoffmann, T. Bertram (2008), *Optimal State Space Control of DC Motor*, Proceedings of the 17th World Congress The International Federation of Automatic Control Seoul, Korea, July 6-11, 2008, IFAC Proceedings, Volume 41, Issue 2, 2008, Pages 5796-5801
6. Masayoshi Tomizuka (1996), *Robust digital motion controllers for mechanical systems*, Robotics and Autonomous Systems, © 1996 Elsevier, 19 (1996) 143-149
7. Mikhov M. (2009), *Mathematical Modeling and Dynamic Simulation of a Class of Drive Systems with Permanent Magnet Synchronous Mo*tors, Applied and Computational Mechanics, Vol. 3, No. 2, pp. 331-338, Czech Republic, 2009, ISSN 1802-680X.
8. Radoslav Vasilev, Dimitar Dimitrov (2012), *Autonomous Mobile Robot for Research and Development of a Perceptual Anchoring System*, Proceedings of the Technical University - Sofia, v. 62, book 2, 2012, ISSN 1311-0829, pp. 313-322
9. Guergov S., Beevski L. (2015), *Study of the Capacity of a Fanuc M430i-A/4FH Robot to Perform Technological Operations*, In Proceedings of Scientific XII International Congress "Machines, Technologies, Materials" 2015, ISSN 1310-3946, Year XXIII, Volume 3 (2015), pp.12-14
10. Vladimir Hristov (2013), *Adaptive Observer of DC Electric Drive*, Proceedings of the Technical University - Sofia, v. 63, book 2, 2013, ISSN 1311-0829, pp. 89-98
11. Xu Chen, Masayoshi Tomizuka (2014), *Transient Enhancement in Add-on Feedforward Algorithms for High-performance Mechatronic Systems*, In Proceedings of the 19th World Congress The International Federation of Automatic Control Cape Town, South Africa. August 24-29, © 2015 Elsevier, 978-3-902823-62-5/2014 © IFAC, 2014, 7214-7220
12. *https://www.robots.com/robots/fanuc-m-430ia-4fh*
13. *http://host118022018037.metio.jp/digianaecatalog/fanuc-430ia/Book/fanuc-430ia-P0000.html*
14. *https://www.flexibleassembly.com/FI-M-430iA-4FH*
15. *https://www.robots.com/images/robots/Fanuc/M-Series/fanuc_M_430IA_4FH_Datasheet.pdf*
16. *https://www.antenen.com/products/industrial-robots/fanuc/501-1400mm/fanuc-m-430ia4fh-r30ia/c-24/c-162/p-16046*
17. *https://www.machinio.com/listings/39560739-fanuc-m430ia-4fh-5-axis-cnc-robot-with-r30ia-controller-in-almont-mi*
18. *https://www.ajsolutions.be/sites/default/files/robot-brochure-en.pdf*
19. *http://robotforum.ru/promyishlennyie-robotyi/fanuc/fanuc-m-430ia-4fh.html*
20. *https://www.fanucamerica.com/docs/default-source/robotics-product-information-sheets/m-430ia-series_17.pdf?sfvrsn=37f0815b_4*